THE PROTEIN SOCIETY

Redox-regulated methionine oxidation of *Arabidopsis thaliana* glutathione transferase Phi9 induces H-site flexibility

Maria-Armineh Tossounian,[1,2,3] Khadija Wahni,[1,2,3] Inge Van Molle,[1,2,3] Didier Vertommen,[4] Leonardo Astolfi Rosado,[1,2,3] and Joris Messens[1,2,3]*

[1]VIB-VUB Center for Structural Biology, Brussels B-1050, Belgium
[2]Brussels Center for Redox Biology, Brussels B-1050, Belgium
[3]Structural Biology Brussels, Vrije Universiteit Brussel, Brussels B-1050, Belgium
[4]de Duve Institute, Université Catholique de Louvain, Brussels B-1200, Belgium

Received 21 February 2018; Accepted 30 April 2018
DOI: 10.1002/pro.3440
Published online 10 July 2018 proteinscience.org

Abstract: Glutathione transferase enzymes help plants to cope with biotic and abiotic stress. They mainly catalyze the conjugation of glutathione (GSH) onto xenobiotics, and some act as glutathione peroxidase. With X-ray crystallography, kinetics, and thermodynamics, we studied the impact of oxidation on *Arabidopsis thaliana* glutathione transferase Phi 9 (GSTF9). GSTF9 has no cysteine in its sequence, and it adopts a universal GST structural fold characterized by a typical conserved GSH-binding site (G-site) and a hydrophobic co-substrate-binding site (H-site). At elevated H_2O_2 concentrations, methionine sulfur oxidation decreases its transferase activity. This oxidation increases the flexibility of the H-site loop, which is reflected in lower activities for hydrophobic substrates. Determination of the transition state thermodynamic parameters shows that upon oxidation an increased enthalpic penalty is counterbalanced by a more favorable entropic contribution. All in all, to guarantee functionality under oxidative stress conditions, GSTF9 employs a thermodynamic and structural compensatory mechanism and becomes substrate of methionine sulfoxide reductases, making it a redox-regulated enzyme.

Keywords: redox; methionine sulfoxide; X-ray structure; methionine sulfoxide reductase; steady-state kinetics; thermodynamics

Abbreviations: AU, asymmetric unit; CDNB, 2,4-Dinitrochlorobenzene; CuOOH, cumene hydroperoxide; FOX assay, ferrous oxidation-xylenol orange assay; GST, glutathione transferase; GSTU23, glutathione transferase Tau23; GSTF9, glutathione transferase Phi9; GSH, glutathione; GSOH, glutathione sulfenic acid; GSSG, glutathione disulfide; GSO_3, glutathione sulfonate; MetSO, methionine sulfoxide; ROS, reactive oxygen species

Additional Supporting Information may be found in the online version of this article.

Word statement: We report the impact of oxidation on the structure and on the active site methionine residues of GSTF9 under hydrogen peroxide stress. Formation of methionine sulfoxide causes an increased flexibility of the active site loop inducing a decrease in its transferase activity, and a decrease of its glutathione peroxidase activity toward hydrophobic substrates. We also show redox regulation of GSTF9 by methionine sulfoxide reductase enzymes, which restore the GSTF9 activity.

Grant sponsor: Vlaams Instituut voor Biotechnologie (VIB); Grant sponsor: Omics@VIB Marie Curie COFUND fellowship; Grant sponsor: FWO PhD Fellowship; Grant sponsor: Fonds voor Wetenschappelijk Onderzoek Vlaanderen; Grant number: G0D7914N; Grant sponsor: Hercules Foundation; Grant number: HERC16; Grant sponsor: Vrije Universiteit Brussel Strategic Research Programm; Grant number: SRP34; Grant sponsor: FWO Excellence of Science Project; Grant number: G0G6918N (EOS ID 30829584).

**Correspondence to*: Joris Messens, VIB-VUB Center for Structural Biology, Redox Signaling lab, Vlaams Instituut voor Biotechnologie (VIB), Vrije Universiteit Brussel (VUB), Pleinlaan 2, 1050 Brussels, Belgium. E-mail: joris.messens@vib-vub.be

Introduction

To understand the global effect of methionine oxidation in plants, we recently identified the sulfoxome (proteome of oxidized methionines) in *Arabidopsis thaliana* leaves exposed to high light stress and we mapped the modifications back to single amino acids, which is key for understanding possible consequences of this post-translational modification on protein function.[1] We found members of the Phi and Tau glutathione transferase (GST) families affected by methionine oxidation.

GST enzymes detoxify electrophilic substrates by glutathione (GSH) conjugation and by peroxide scavenging.[2,3] Particularly, they are involved in the detoxification of heavy metals[4] and herbicides.[5] Some GST members deglutathionylate their substrates,[6] and others are involved in cell signaling by interacting with substrates that have an important signaling role.[7] The *A. thaliana* genome encodes for 55 GST enzymes, which are differently expressed and regulated depending on the type of biotic and abiotic stress conditions.[4] GST enzymes are subdivided into different classes depending on their amino acid sequence, catalytic residues (Ser, Tyr, or Cys), and their tertiary structure.[8,9] Although members of the plant GST classes have low primary sequence identity, they share an overall common structural fold.[5,10,11]

Most cytosolic GST enzymes are homodimeric and have an N-terminal thioredoxin-like domain, which contains the glutathione (GSH) binding site (G-site) and a C-terminal alpha-helical domain, which contains the hydrophobic substrate-binding site (H-site).[8] Upon GSH binding to the G-site, the catalytic residue (Ser, Tyr, or Cys), which is Ser for Phi and Tau class GSTs, activates GSH (thiol) to GS^-(thiolate), which is then conjugated to an electrophilic substrate located within the H-site via a thio-ether bond.

Some GST enzymes contain cysteines, located close to the active site, which are highly sensitive to oxidation. For example, we recently showed that *A. thaliana* GSTU23 forms a reversible disulfide that protects against oxidative damage.[12] Other GST enzymes have no cysteines, like some of the Phi class members, where methionine residues play a role in redox regulating their transferase activity.[13]

Here, we present the impact of oxidation on the structure and function of GSTF9, an enzyme with no cysteines. GSTF9 is constitutively expressed together with GSTF10, GSTU5, and GSTU13, indicating its importance as housekeeping enzyme.[14] Further, Horvath et al. showed that an *A. thaliana* GSTF9 loss-of-function mutant has a decreased overall glutathione peroxidase activity.[15] We found that the oxidation of methionines located near or within the G- and H-sites of GSTF9 lead to increased flexibility of the H-site loop, which results in a decrease in the affinity for the substrates, GSH and CDNB. Upon oxidation, GSTF9 glutathione peroxidase activity decreases for the more hydrophobic peroxides.

Results

GSTF9 has a universal GST structural fold

This study focuses on the impact of oxidation on the structure and function of *A. thaliana* glutathione transferase Phi 9 (GSTF9), which was identified within the list of the proteins with an oxidized methionine, the *A. thaliana* sulfoxome.[1] Reduced GSTF9 ($GSTF9_{red}$) was purified to homogeneity and crystallized using the hanging drop vapor diffusion method. We solved the structure to a resolution of 2.34 Å (PDB code 6EZY) (Table I). As observed for other GSTs, $GSTF9_{red}$ is a homodimer and forms trigonal crystals, with one $GSTF9_{red}$ dimer in the asymmetric unit. Each monomer contains a thioredoxin domain followed by an α-helical domain (Fig. 1). The thioredoxin domain contains the glutathione (GSH) binding site (G-site), while the hydrophobic substrate binding site (H-site) is embedded within the C-terminal helical bundle domain. The G-site shows a high degree of structural conservation, while the conservation of the H-site is rather limited.[16] The catalytic Ser12 within the G-site is responsible for GSH activation (Fig. 1). We observed a GSH molecule residing the G-site of the $GSTF9_{red}$ structure, while the H-site is occupied by glutathione sulfenic acid (GSOH) (Fig.1). The presence of two GSH molecules, or even a glutathione disulfide (GSSG) has been shown previously for the *E. coli* Nu class of GST enzymes.[17,18] Overlay of these structures with the $GSTF9_{red}$ structure shows that the GSH molecules in YghU and YfcG are differently oriented.

Oxidation impacts transferase activity but not H_2O_2 peroxidase activity

GSTF9 belongs to the Phi class of glutathione transferases, for which both glutathione transferase and peroxidase activities have been described.[14,19] To study the impact of oxidation on transferase and peroxidase activities (Fig. 2), $GSTF9_{red}$ was oxidized with H_2O_2 (1:100 molar ratio) to obtain $GSTF9_{ox}$, followed by oxidant removal. The transferase activity of GSTF9 was measured by monitoring the increase of absorbance at 340 nm for the conjugation of the thiol group of GSH to the CDNB substrate in function of time. The initial velocities were plotted for several conditions [Fig. 2(A)]. As previously reported by Jacques et al.,[1] we observed a 30% decrease in initial velocity for $GSTF9_{ox}$ [Fig. 2(A)]. To study the influence of oxidation on the glutathione peroxidase activity of GSTF9, we used a FOX

Table I. *GSTF9 X-Ray Data Collection and Refinement Statistics*

Dataset PDB code	$GSTF9_{red}$ 6EZY	$GSTF9_{H2O2+NaOCl}$ 6F01	$GSTF9_{ox}$ 6F05
Data collection			
Beamline	IO4@DLS	IO4@DLS	IO4@DLS
Wavelength	0.9795	0.9795	0.9795
Processing			
Space group	P31 2 1	P31 2 1	P1
Cell parameters (Å/°)	61.43 93.97 107.71 93.19 101.57 101.97	114.76 114.76 90.31 90 90 120	61.43 93.97 107.71 93.19 101.57 101.97
Resolution, Å (outer shell)[a]	48.13–2.34 (2.48–2.34)	66.84–2.5 (2.57–2.5)	62.7–2.2 (2.26–2.2)
Total reflections	282,989 (43,703)	158,033 (11,796)	268,584 (19,908)
Unique reflections	2880 (4594)	24179 (1781)	116579 (8561)
Completeness (%)	98.7 (96.8)	99.8 (99.9)	97.8 (97.1)
Multiplicity	9.9 (9.5)	6.5 (6.6)	2.3 (2.3)
CC1/2 (%)	99.9 (55.9)	99.5 (71.1)	99.7 (73.3)
Rmeas (%)	11.2 (137.9)	17.7 (124.8)	7.4 (60.4)
$<I/\sigma(I)>$	18.3 (1.64)	11.56 (2.09)	10.67 (2.08)
Refinement			
Resolution range (Å)	49.41–2.35	66.84–2.3	65.73–2.06
Percentage observed (%)	98.79	99.84	97.66
R_{cryst} (%)[b]	15.63	16.43	16.15
R_{free} (%)[c]	19.66	20.89	20.93
RMS			
Bonds (Å)	0.012	0.010	0.008
Angles (°)	1.267	1.268	1.18
Ramachandran plot			
Most favored (%)	97.83	97.31	97.76
Additionally allowed (%)	1.69	2.2	1.68
Disallowed (%)	0.48	0.49	0.56
Bound ligand	GSH (G-site) and GSOH (H-site)	GSO_3 (G-site) and GSOH (H-site)	GSO_3 (G-site)

[a] Values between brackets are for the highest resolution shell.
[b] $R_{cryst} = \Sigma||F_{obs}| - |F_{calc}||/\Sigma|F_{obs}|$, F_{obs} and F_{calc} are observed and calculated structure factor amplitudes.
[c] R_{free} is the same as R_{cryst}, but using a random subset of 5% of the data excluded from the refinement.
DLS, diamond light source.

assay [Fig. 2(B)]. Progress curves [Fig. 2(B)] show that $GSTF9_{red}$ and $GSTF9_{ox}$ remove H_2O_2 with similar rates.

G- and H-site methionines form a sulfoxide

In our previous study on GSTF9,[1] we reported sulfur oxidation of Met35, which is located close to the G-site (Fig. 1). We decided to determine whether the methionines (Met35, Met118, and Met123) located within or near the G- and H- sites of GSTF9 could influence its activity upon hydrogen peroxide treatment (Fig. 1). Therefore, both $GSTF9_{red}$ and $GSTF9_{ox}$ samples were trypsin or chymotrypsin digested, and the formation of methionine sulfoxide and sulfone was analyzed by mass spectrometry. We found sulfoxide and sulfone formation on Met35 (Fig. 3), which is located close to the G-site, and sulfoxide on Met118 and Met123, which are located close to the H-site (Fig. 1). Aside from the active site methionines, also Met184, which is surface exposed and located at the opposite side of the active site, was oxidized to methionine sulfoxide. Taken its location at distance of more than 18 Å away from the active site Ser12 (Fig. 1), it is highly unlikely that Met184 oxidation would directly influence the activity of GSTF9.

Oxidized GSTF9 is a methionine sulfoxide substrate

As methionine oxidation causes a decrease in the transferase activity of GSTF9 [Fig. 2(A)], we wondered whether the transferase activity could be recovered by methionine sulfoxide reductase. Therefore, we incubated 10 μM $GSTF9_{ox}$ with a 5 μM mixture of methionine sulfoxide reductase A (MsrA) and B (MsrB) for 1 h at 25°C, and measured the initial velocity in the CNDB-GSH conjugation assay. The drop in transferase activity seen for $GSTF9_{ox}$ was almost completely recovered [Fig. 2(A)], which indicates that Msr enzymes regulate the activity of GSTF9 under oxidative stress conditions.

Oxidation has only a marginal effect on the specificity constants

Next, we wanted to understand the impact of oxidation on the kinetic parameters of GSTF9, and this for both the G-site binding GSH substrate and the H-site binding CDNB substrate (Table II and

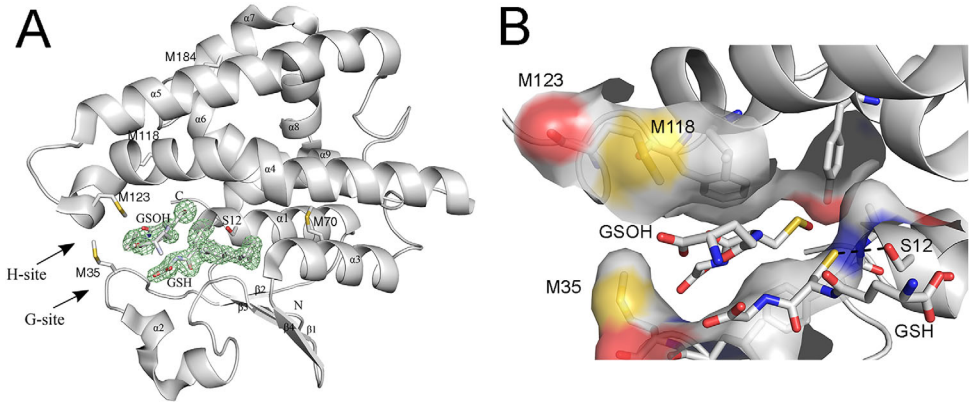

Figure 1. Crystal structure of reduced GSTF9. (A) The X-ray crystal structure of reduced $GSTF9_{red}$ shows a typical GST-fold. The crystal structure of $GSTF9_{red}$ is shown in a gray cartoon representation with the alpha helices and beta sheets labeled. The glutathione (GSH) binding site (G-site) and the hydrophobic substrate-binding site (H-site) are indicated with arrows. A glutathione molecule is observed in the G-site, and sulfenylated GSH (GSOH) in the H-site. The catalytic serine (S12), the Met residues (M35, M70, M118, M123 and M184), and the N- and C-terminus are indicated. An omit map contouring the GSH and GSOH at 3σ is shown in green. (B) A closer view of the three methionines (M35, M118 and M123) located close to the G- and H-site. Surface representation is shown for atoms within 4 Å of H-GSOH. The H-bond between the catalytic S12 and the sulfur of GSH is 3.3 Å (black dotted line).

Supporting Information, Fig. S1). From the Michaelis–Menten curves (Supporting Information, Fig. S1) under respective substrate saturating conditions, we determined K_M and k_{cat} values. GSTF9 oxidation increased the K_M for CDNB from 1.3 to 1.8 mM, but the k_{cat} only slightly varies from 0.98 to 0.72 s^{-1}. For GSH, the K_M decreases twofold from 131 μM to 71 μM, while the k_{cat} only slightly varies from 0.85 to 0.5 s^{-1}. The overall effect of oxidation on k_{cat}/K_M is only marginal as the specificity constants are

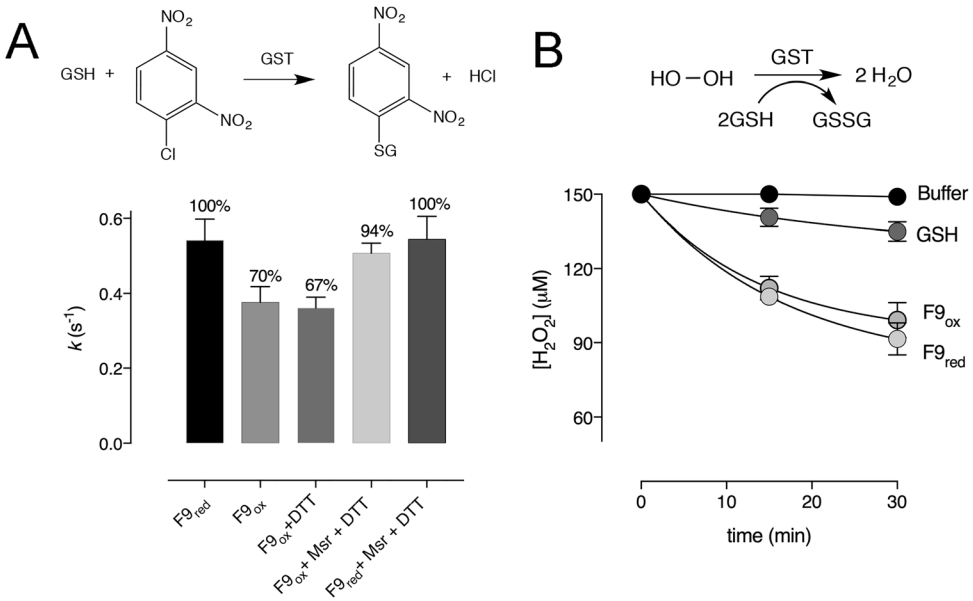

Figure 2. GSTF9 oxidation has a different impact on the transferase and glutathione peroxidase activity. (A) Bar graphs show the percentage of transferase activity measured in rate constants (k) of $GSTF9_{red}$ and $GSTF9_{ox}$ (0.2 μM), where the GST catalysed conjugation of GSH (0.5 mM) onto CDNB (3.8 mM) is followed at 340 nm. When oxidized, $GSTF9_{ox}$ activity significantly ($P < 0.001$) decreases from 100% (0.54 s^{-1}) to 70% (0.38 s^{-1}). MsrA and MsrB treatment causes activity increase from 70% to 94% (0.51 s^{-1}), indicating that Msr enzymes are capable of recovering $GSTF9_{ox}$ activity. Two control samples were used: $GSTF9_{ox}$ incubated with DTT and $GSTF9_{red}$ incubated with MsrA, MsrB and DTT. The data from at least 3 independent experiments are presented as a mean ± SD. (B) FOX assay was used to compare the peroxidase activity of $GSTF9_{red}$ and $GSTF9_{ox}$ in the presence of 150 μM H_2O_2. Remained H_2O_2 concentrations were determined for samples taken after 15 and 30 min. Upon treatment of GSTF9 with hydrogen peroxide ($GSTF9_{ox}$), glutathione peroxidase activity is not influenced. As a control, the influence of GSH on H_2O_2 reduction was also recorded. The data from 3 independent experiments were normalized and presented as a mean ± SD.

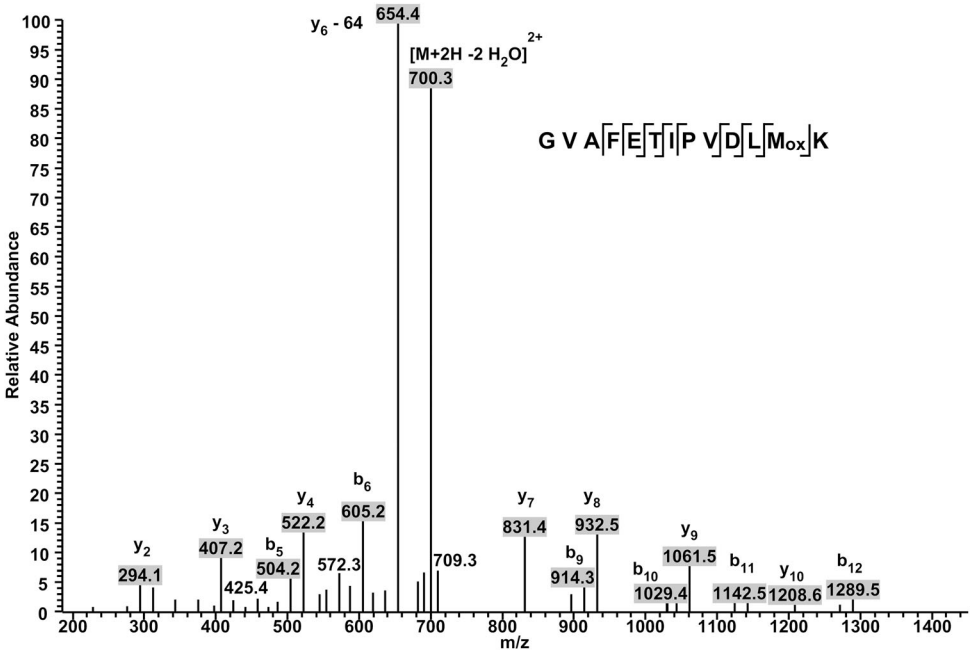

Figure 3. Identification of Met35 of GSTF9 as a methionine sulfoxide. Identification of oxidation on Met35 of GSTF9 under H_2O_2 exposure. The LC-MS spectrum shows MS^2 data obtained from a +2 parent ion with m/z 718.3. The y- and b- series of ions allow exact localization of the methionine sulfoxide. A neutral loss of 64 Da is observed from the y_6 daughter ion and corresponds to the release of methane sulfenic acid (CH_3SOH) from the side chain of methionine sulfoxide.

within the same range, $\sim 10^2$ M^{-1} s^{-1} for CDNB and $\sim 10^3$ M^{-1} s^{-1} for GSH (Table II).

GSTF9 oxidation induces H-site flexibility

To understand the impact of oxidation at the molecular level, we decided to solve the structure of oxidized GSTF9 crystals. First, crystals were grown using $GSTF9_{ox}$ (GSTF9 oxidized using a 1:100 GSTF9:H_2O_2 ratio). The resulting $GSTF9_{ox}$ structure was solved to 2.2 Å resolution (Table I, PDB code 6F05). Second, we exposed the $GSTF9_{red}$ crystals to the extreme oxidation conditions of 0.5 M H_2O_2 and 1 mM NaOCl for 1 h ($GSTF9_{H2O2+NaOCl}$, PDB code 6F01). While $GSTF9_{red}$ (Fig. 1) formed trigonal crystals, the $GSTF9_{ox}$ formed triclinic crystals (Table I), with 10 copies of GSTF9 in the asymmetric unit (AU). Overlay of all the chains of $GSTF9_{ox}$ and $GSTF9_{H2O2+NaOCl}$ clearly shows mobility of the Met35, Met118 and M123 side chains, and also the electron density surrounding amino acids 120–127 is absent in all the 10 copies in the AU [Fig. 4(A)]. Unfortunately, within the crystal structures of the oxidized GSTF9, $GSTF9_{ox}$ and $GSTF9_{H2O2+NaOCl}$, the side chain of Met35 was not always well defined, as it is localized on a highly mobile loop between the β2-strand and the α2-helix (amino acids 34–43). In the structures of both oxidized GSTF9, $GSTF9_{ox}$ and $GSTF9_{H2O2+NaOCl}$, the Met35, Met118, and Met123 sulfurs do not show any sulfoxide or sulfone formation under the applied oxidation conditions [Fig. 4(A)], which is different from what we observed in our mass spectrometric results.

Glutathione sulfonate (GSO_3) inhibits the transferase activity

In addition to the high loop mobility close to the active site in both oxidized GSTF9 structures, $GSTF9_{H2O2+NaOCl}$ and $GSTF9_{ox}$, we observed GSH oxidized to glutathione sulfonate (GSO_3) within the G-site. GSO_3 is bound in exactly the same orientation as GSH in the G-site [Fig. 4(B,C)]. Both the GSH and GSO_3 γ-Glu moieties hydrogen bond to Glu65 and Ser66. The glycyl moieties hydrogen bond

Table II. *Steady-State Kinetics Parameters of GSTF9 Under Reducing and Oxidizing Conditions*

	[GSH]		[CDNB]	
	$F9_{red}$	$F9_{ox}$	$F9_{red}$	$F9_{ox}$
K_M	131 ± 9 μM	71 ± 7 μM	1.3 ± 0.1 mM	1.8 ± 0.2 mM
k_{cat} (s^{-1})	0.85 ± 0.02	0.50 ± 0.01	0.98 ± 0.02	0.72 ± 0.04
k_{cat}/K_M ($M^{-1}s^{-1}$)	6.5×10^3	7.0×10^3	7.5×10^2	4.0×10^2

Kinetic parameters were determined using varying concentrations of GSH or CDNB and the values were plotted using the Michaelis–Menten equation.

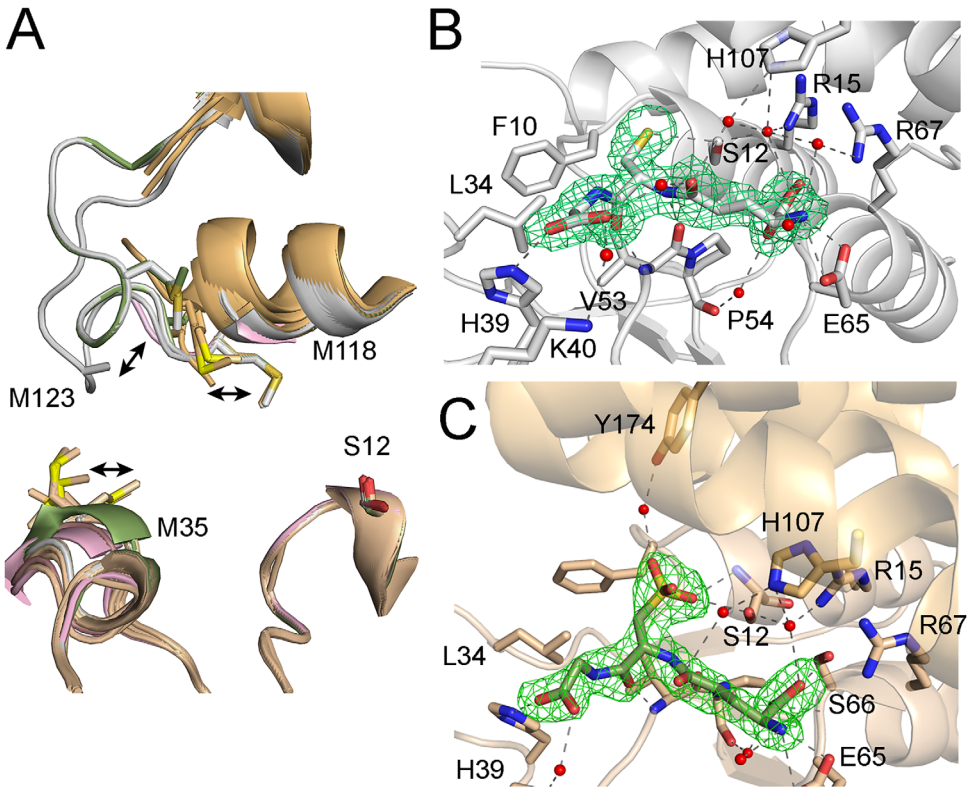

Figure 4. Oxidation leads to GSTF9 H-site disorder and oxidized glutathione (GSO_3) formation in the G-site. (A) Overlay of the 10 copies of GSTF9 in the AU of $GSTF9_{ox}$ (shown in gold cartoon) and the two chains present in the AUs of both the $GSTF9_{red}$ (chain A and B in gray cartoon) and $GSTF9_{\_H2O2+NaOCl}$ structures (chain A in pink, chain B in green) shows a high mobility for the α2-β2 and especially the α4-α5 loops. Residues 120–127 in the latter loop become entirely disordered in the $GSTF9_{ox}$ structure, as well as in chain A of the $GSTF9_{\_H2O2+NaOCl}$ structure. The side chains of Met35, Met118 and Met123 shown in sticks are highly mobile. (B-C) The active site H-bond network of $GSFT9_{red}$ (gray cartoon) has a GSH molecule (B), which is oxidized to GSO_3 (C) within the $GSTF9_{ox}$ G-site (gold cartoon). The residues (gold for $GSTF9_{ox}$ and gray for $GSTF9_{red}$) interacting with GSH and GSO_3 are shown in stick representation. Leu34 and Phe10 delineate the G-site. Hydrogen bonds are in gray or black dashed lines. Water molecules H-bonded to GSH or GSO_3 are in red spheres. An omit map contouring the ligands, GSH and GSO_3, at 3σ is shown in green.

to His39 and via a water molecule to Lys40. Where the GSH Cys sulfur interacts with the Ser12 OH group [Figs. 1(B) and 4(B)], the SO_3 group of GSO_3 makes hydrogen bonds with the Ser12 OH group, as well as with the Ser12 backbone. Via a water molecule it also interacts with the side chain of Tyr174 [Fig. 4(C)]. The GSH and GSO_3 seem to be strongly bound to the G-site as all the size exclusion chromatography attempts to remove the GSH from GSTF9 were unsuccessful.

As a molecule of glutathione sulfonate (GSO_3) resides in the active site of $GSTF9_{ox}$ and $GSTF9_{H2O2+NaOCl}$, we decided to test the effect of GSO_3 on GSTF9 transferase activity. GSTF9 was incubated with increasing concentrations of GSO_3 (0–300 μM), and the transferase activity was measured. The increase in GSO_3 concentration led to a decrease of the transferase activity with an inhibition constant (K_i) of 34 μM [Fig. 5(A)]. Hence, formation of GSO_3 during the oxidation of GSTF9 could be another reason for the decrease in transferase and peroxidase activity [Fig. 5(B)].

$GSTF9_{ox}$ reduces hydrophobic peroxides less efficiently

Next, we decided to test whether increased H-site flexibility observed within $GSTF9_{ox}$ might be the reason for the decreased transferase activity. Loss of a structured H-site under oxidative stress [Fig. 4(A)] might affect the binding of hydrophobic substrates in the H-site of GSTF9. The CDNB molecule used in the transferase assay is a hydrophobic molecule as it contains a benzene ring that needs to be correctly oriented in the H-site for GSH transfer. Therefore, we decided to test the $GSTF9_{red}$ and $GSTF9_{ox}$ peroxidase activity with two hydrophobic peroxides: cumene hydroperoxide (with a benzene ring) and tert-butyl hydroperoxide (with a more extended carbon chain) (Fig. 6, Table III, and Supporting Information). The results show a similar glutathione peroxidase activity for $GSTF9_{red}$ and $GSTF9_{ox}$ towards H_2O_2 after 30 min incubation (Fig. 6 and Supporting Information, Table SI). On the other hand, when comparing the $GSTF9_{red}$ and $GSTF9_{ox}$ peroxide reduction after 30 min incubation with

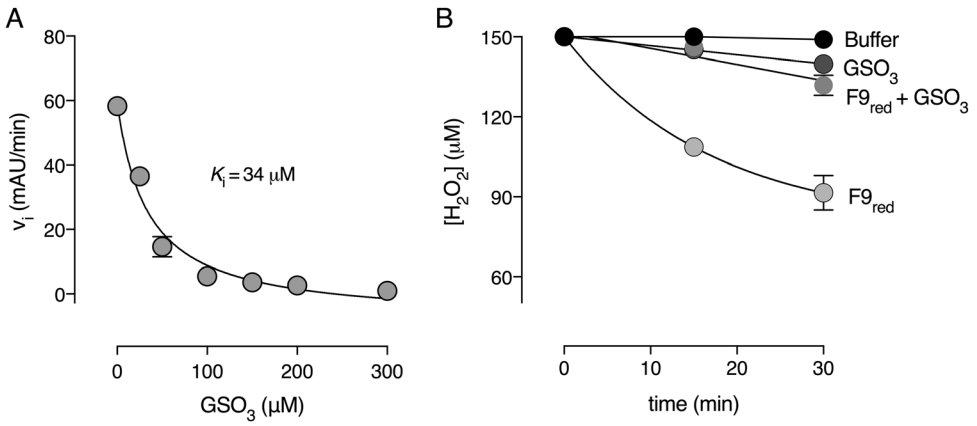

Figure 5. Glutathione sulfonate (GSO_3) inhibits GSTF9 glutathione transferase and peroxidase activity. Increasing concentrations of GSO_3 results in a decrease of the initial velocity of (A) the GSTF9 glutathione transferase and (B) the peroxidase activity. The inhibition constant (K_i) for the transferase activity is 34 μM. The data represent the mean ± SD of 2 independent experiments.

tert-butyl peroxide and cumene hydroperoxide, it became apparent that less peroxide is being consumed for these more hydrophobic peroxides by $GSTF9_{ox}$ (Table III and Supporting Information). A clear trend was observed, peroxidase activity towards more hydrophobic peroxides decreases for $GSTF9_{ox}$ compared to $GSTF9_{red}$ (Fig. 6). The correlation between the concentration of peroxide consumed by $GSTF9_{red}$ versus the hydrophobicity index (ALogP) of the peroxides corroborates the hypothesis that GSTF9 oxidation impairs its activity towards hydrophobic substrates (Fig. 6).

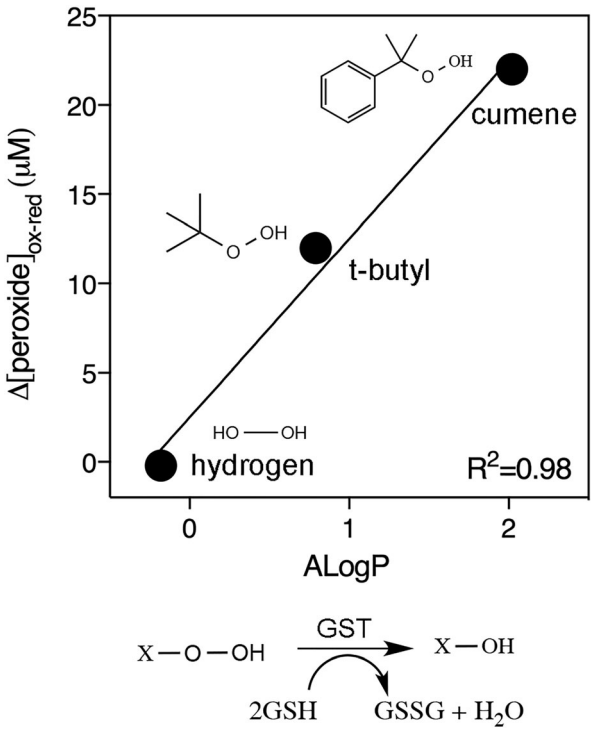

Figure 6. Oxidized GSTF9 reduces hydrophobic peroxides less efficiently. A difference plot of the peroxide concentration (μM) (H_2O_2, t-butyl peroxide, CuOOH) reduced after 30 min with $GSTF9_{ox}$ and $GSTF9_{red}$ versus the hydrophobicity index (ALogP) of the peroxides is presented. The more hydrophobic the peroxide, the larger the difference between $GSTF9_{red}$ and $GSTF9_{ox}$ peroxide reduction (Δ[peroxide]). The data represent the mean ± SD of 3 independent experiments. The reduction scheme for peroxides (X) with the release of oxidized glutathione (GSSG) and a water molecule is shown. The structures of the three peroxides (H_2O_2, t-butyl peroxide, CuOOH) are generated using ChemBioDraw 14.0.

$GSTF9_{ox}$ employs a thermodynamic compensatory system

To further understand the source of the increased structural flexibility observed upon GSTF9 oxidation, we decided to compare the thermodynamic activation parameters ($\Delta H^{\#}$, $\Delta S^{\#}$, and$\Delta G^{\#}$) and the energy of activation (E_a) of oxidized and reduced GSTF9. Therefore, we determined the initial velocities of the transferase activity with CDNB at different temperatures. We derived the thermodynamic parameters of the CDNB glutathione transferase reaction from the linear Eyring and Arrhenius plots and the respective equations (Table IV and Fig. 7). We observed an enthalpy–entropy compensatory system where changes in enthalpy are balanced by changes in entropy, leading to similar $\Delta G^{\#}$ values for $GSTF9_{red}$ and $GSTF9_{ox}$.[20] The energy of activation (E_a) and enthalpy ($\Delta H^{\#}$) values indicate a larger energetic barrier to be overcome by oxidized GSTF9 compared to reduced GSTF9. The increased energy barrier is accompanied by a less pronounced conformational change of $GSTF9_{ox}$ to reach the activated complex, leading to this enthalpy–entropy compensatory mechanism.

Discussion

Glutathione transferase (GST) enzymes play an important role in the protection of plants against different stress conditions including xenobiotic and

Table III. *Glutathione Peroxidase Activity of GSTF9$_{red}$ and GSTF9$_{ox}$ Using Different Peroxides*

	Time (min)	[H_2O_2] (μM)	[t-butyl peroxide] (μM)	[CuOOH] (μM)
$F9_{red}$	0	200 ± 0	200 ± 0	200 ± 0
	15	171 ± 1	180 ± 4	117 ± 4
	30	161 ± 2	162 ± 7	84 ± 9
$F9_{ox}$	0	200 ± 0	200 ± 0	200 ± 0
	15	163 ± 0	191 ± 4	147 ± 7
	30	162 ± 1	174 ± 0	106 ± 7

The concentration of peroxide present within the sample containing GSTF9$_{red}$ and GSTF9$_{ox}$ with 1 mM GSH at time 0, 15, and 30 min is shown.

peroxide stress.[3,21] Understanding how these enzymes function and how their activities are influenced under stress conditions is important to understand how they survive extreme conditions. Prior to this study, two members of the GST family, GSTU23 and GSTF9, were found present in the sulfoxome of *A. thaliana* leafs exposed to high light stress,[1] and as such sensitive to methionine oxidation. In a recent study, we have investigated how the activity of GSTU23 is influenced under hydrogen peroxide stress.[12] We found that at lower H_2O_2 levels (100 μM), MetSO formation is the major post-translational modification on GSTU23, which is recycled by methionine sulfoxide reductases (Msr). Here, we focus on the impact of oxidation on GSTF9, an enzyme with no cysteines.

GSTF9 has no cysteines, but six methionines, three of which (Met35, Met118, and Met123) are located within or close to the G- and H-sites (Fig. 1), and which could interfere with GSH or hydrophobic substrate binding. We showed with mass spectrometry sulfoxidation of these three methionines and how they influence the GSTF9 glutathione transferase activity [Fig. 2(A)] and the glutathione peroxidase activity [Fig. 2(B), 6]. A similar case is observed in a study performed by Lee et al.,[13] where oxidation of methionines in *A. thaliana* GSTF2 and GSTF3 causes a decrease in the GST transferase activity, and this activity could be recovered with methionine sulfoxide reductase B7 (MsrB7). Important to note is that similar to GSTF9, both GSTF2 and GSTF3 also contain no Cys residues.[13] Similarly, we showed a decrease in glutathione transferase activity of *A. thaliana* GSTU23 upon methionine oxidation, which is restored when treated with MsrA and MsrB.[12] Here, we show the importance of MsrA and MsrB in restoring GSTF9 transferase activity [Fig 2(A)]. Treatment with the Msr enzymes recovers the transferase activity of GSTF9$_{ox}$ up to 94%; however, 6% remains unrecovered. This might be due to the presence of a methionine sulfone, as observed in the MS analysis, or the presence of GSO_3, which was observed in the active site of GSTF9$_{ox}$ structure [Fig. 4(C)].

The active site of GST enzymes consists of a highly conserved GSH binding site, also known as the G-site, and a less conserved hydrophobic H-site, which coordinates the binding of the hydrophobic co-substrates to which GSH is transferred.[22] Mechanistically, H-bonding of GSH with a catalytic Ser residue of the G-site results in a drop of the sulfur pK_a,[23–25] stabilizing it as a thiolate for a nucleophilic attack on an electrophilic co-substrate in the H-site.[26] To find out how methionine sulfoxide modifications could interfere with the binding of the substrates to both active sites, we determined the steady-state kinetic parameters by varying both substrates concentrations (GSH and CDNB) (Table II and Supporting Information, Fig. S1). The results show especially an increase in the K_M for CDNB, and a decrease of the K_M for GSH, with less variation in the k_{cat} values (Table II). GSTF9 does not use a K_M–k_{cat} compensatory mechanism to deal with increased H_2O_2 concentrations as observed for *A. thaliana* GSTU23,[12] or for cytosolic malate dehydrogenase 1 (MDH1).[27]

We clearly observed increased flexibility of the loop carrying Met35 (between β2 and α2) [Fig. 4(A)], located close to the G-site, and the loop carrying Met118 and Met123 (between α4 and α5), located at the H-site [Fig. 4(A)]. Although methionine oxidation was observed with mass spectrometry and we showed activity recovery with methionine sulfoxide reductases, methionine sulfoxide formation was not observed in the structures, as electron density for the α4–α5 loop is missing in the oxidized structures. Oxidation of protein methionines, which lead to local unfolding and impact the protein activity, have been reported in several other studies.[28,29] For example, the chaperone-like activity of *A. thaliana* chloroplast Hsp21 is influenced due to the oxidation of its N-

Table IV. *Thermodynamic Activation Parameters for CDNB Glutathione Transferase Activity with Reduced and Oxidized GSTF9*

	E_a (kcal mol^{-1})	$\Delta H^{\#}$ (kcal mol^{-1})	$T\Delta S^{\#}$ (kcal mol^{-1})	$^{a}\Delta G^{\#}$ (kcal mol^{-1})	$\Delta(\Delta H^{\#})_{ox\text{-}red}$ (kcal mol^{-1})	$\Delta(T\Delta S^{\#})_{ox\text{-}red}$ (kcal mol^{-1})	$\Delta(\Delta G^{\#})_{ox\text{-}red}$ (kcal mol^{-1})
GSTF9$_{red}$	9.4 (±0.5)	8.8 (±0.5)	−9.0 (±0.9)	17.9 (±1)	2.3	2	0.3
GSTF9$_{ox}$	11.7 (±0.6)	11.1 (±0.6)	−7.0 (± 0.6)	18.2 (±1)			

[a] $\Delta G^{\#}$ was calculated at 25°C.

$\Delta(\Delta H^{\#})_{ox\text{-}red}$ and $\Delta(T\Delta S^{\#})_{ox\text{-}red}$ represent the variation of the thermodynamic parameters between GSTF9$_{ox}$ and GSTF9$_{red}$.

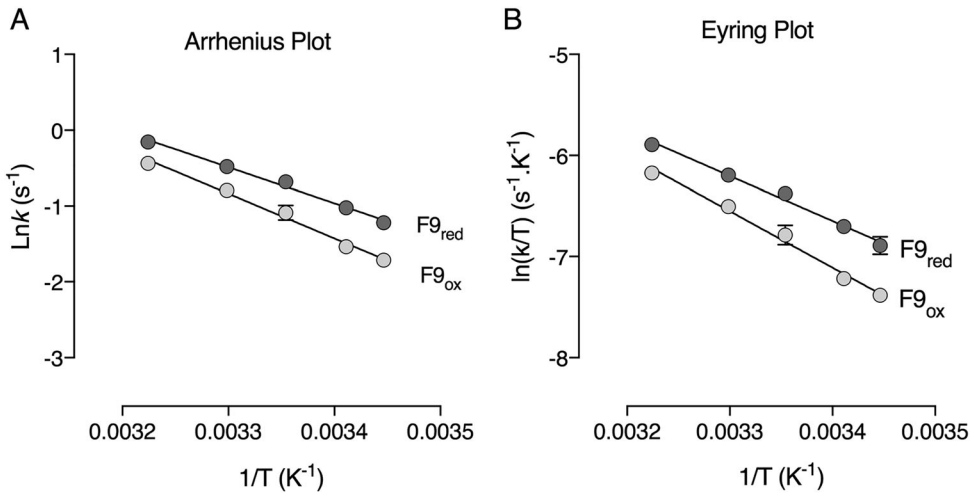

Figure 7. Arrhenius (A) and Eyring (B) plot of $GSTF9_{red}$ and $GSTF9_{ox}$. Temperature dependence of ln*k* and ln (*k*/T) of the glutathione transferase catalyzed reaction by reduced and oxidized GSTF9 at pH 6.4 in a temperature range from 17°C to 37°C is shown. The linearity of the plots suggests that there is no change in the rate-limiting step or protein inactivation within this temperature range.

terminal methionines (Met49, Met52, Met55, and Met59). Here, methionine sulfoxide formation causes partial unfolding due to the local loss of the helical structure.[28] For GSTF9, it looks that methionine oxidation induces local flexibility of the loops between β2–α2 and between α4–α5, which could make these loops more accessible to the *A. thaliana* MsrA or MsrB, and thus facilitating sulfoxide reduction.

Numerous glutathione transferase enzymes can also act as hydroxyl peroxidases but with rate constants much lower[30,31] than those for established glutathione peroxidases and peroxiredoxins.[32,33] While oxidation has been shown to decrease the H_2O_2 peroxidase activity of GSTU23,[12] our results show that the GSTF9 glutathione peroxidase activity is resistant to oxidation. However, the glutathione peroxidase activity of $GSTF9_{ox}$ is more impaired for hydrophobic peroxides (Table III, Supporting Information, SI, and Fig. 6). This suggests that the loss of a structured hydrophobic H-site upon oxidation of GSTF9 forms the basis for the loss in peroxidase activity toward more hydrophobic peroxides.

To further understand the observed changes in kinetic efficiency of GSTF9, we studied the transition state thermodynamic parameters of reduced and oxidized GSTF9 (Fig. 7 and Table IV). To study the transition state of $GSTF9_{red}$ and $GSTF9_{ox}$, thermodynamic parameters were calculated and the data of the activated complex show a compensatory system with different enthalpy and entropy values for oxidized and reduced GSTF9 (Table IV). Generally, when comparing both forms, the overall spontaneity of the $E{:}S^{\#}$ formation is similar (reflected by similar $\Delta G^{\#}$ values), but a different intermediate transition state along the reaction coordinates might get temporally populated. The E_a and $\Delta H^{\#}$ are a result of the sum of interatomic interactions that undergo rearrangement during the E:S activation step. These interatomic interactions are hydrogen bonds and van der Waals interactions between enzyme and substrates.[34] A positive difference of 2.3 kcal/mol was found when the absolute value of $\Delta H^{\#}$ of the oxidized GSTF9 was subtracted from the $\Delta H^{\#}$ value obtained for its reduced counterpart. The less pronounced energetic barrier for $GSTF9_{red}$ indicates that the number of interactions that needs to be rearranged in the reduced form is smaller than in the oxidized form (Table IV), leading to the observed energetic difference. Subsequently, the E:S complex formed by the reduced form seems to be less pronounced and more prone to rearrangement to achieve the transition state. Entropy is the measure of the number of microstates available for a specific species and is more widely described as the degree of disorder. The generation of disorder when E:S is converting to $E{:}S^{\#}$ comes from bond rearrangement and changes in solvation.[35] The value obtained for $\Delta(T\Delta S^{\#})_{ox\text{-}red}$ indicates that $GSTF9_{red}$ undergoes a larger conformational change to reach the transition state when compared with $GSTF9_{ox}$.[36] The more positive $T\Delta S^{\#}$ and positive $\Delta H^{\#}$ indicates that the increased flexibility of the loops between β2–α2 and between α4–α5 is a positive feature, and to achieve the transition state a larger number of interatomic interactions need to be rearranged. Accordingly, to maintain its enzymatic activity under oxidative stress, GSTF9 seems to follow a structural compensatory system. The best scenario is composed by an increase in flexibility in the regions directly involved in catalysis and an increase in rigidity in all the other areas; however, GSTF9 oxidation increased the flexibility globally, leading to a neglectable $\Delta(\Delta G^{\#})_{ox\text{-}red}$ value.[36]

In conclusion, we showed that methionine oxidation near the two active sites causes local loop-flexibility. As a consequence, oxidized GSTF9 becomes substrate for methionine sulfoxide reductases. By thermodynamic and structural compensatory mechanisms, GSTF9 has evolved to become an enzyme that is able to catalyze detoxification reactions under oxidative conditions.

Materials and Methods

GSTF9 purification and oxidation

Protein expression, purification, and oxidation were performed as described by Jacques et al.[4] Prior to oxidation, GSTF9 was reduced with 10 mM DTT at RT for 30 min followed by gel filtration using a Superdex75 HR 10/30 size exclusion chromatography (SEC) column equilibrated in 1× PBS. The collected sample was incubated with 1:100 molar ratio of protein to H_2O_2 for 135 min at 10°C, as performed by Jacques et al.[4] Micro Bio-Spin® Chromatography Column (BIO-RAD) equilibrated with 1× PBS was used to remove excess of H_2O_2.

Glutathione transferase activity assay

The assay was performed as described by Habig et al.[37] Briefly, a UV–visible Varian Cary 100 spectrophotometer was used to measure the GSTF9 catalyzed conjugation of GSH onto CDNB at A_{340}. The reaction mixture was composed of 0.5 mM GSH and 0.2 μM GSTF9 in 250 mM MOPS pH 6.5 and 150 mM NaCl buffer. The assay was initiated by the addition of 3.8 mM CDNB to a final reaction volume of 500 μL.

To determine the influence of Msr incubation on the $GSTF9_{ox}$ transferase activity, a 2:1 molar ratio of $GSTF9_{ox}$ (10 μM) was incubated with *Corynebacterium diphtheriae* MsrA[38] or MsrB[12] (5 μM) for 1 h at 25°C in a 1× PBS buffer containing 0.5 mM DTT. As a control, $GSTF9_{red}$ was also incubated with MsrA, MsrB and DTT. The samples were diluted and 10 μL was transferred to the assay mixture (500 μL), where the final concentrations were: 0.2 μM GSTF9, 0.1 μM Msr, and 10 μM DTT. A sample with only $GSTF9_{ox}$ and DTT was included as a control. Prior to the incubation of GSTF9 with Msr enzymes, both MsrA and MsrB were incubated with 20 mM DTT for 30 min at room temperature. Following reduction, DTT was removed on a Micro Bio-Spin® Chromatography Column (BIO-RAD) equilibrated with 1× PBS.

To determine the kinetic parameters of GSTF9, at varying concentrations of GSH (0–750 μM) or CDNB (0–4.5 mM) the initial velocities were measured and the Michaelis–Menten Eq. (1) was used to fit these data and obtain the kinetic parameters k_{cat} and K_M. For varying [GSH], the CDNB concentration used was 3.8 mM and for varying [CDNB], 0.5 mM GSH was used. Two independent replicates were measured for each substrate concentration. In Eq. (1), v represents the initial velocity, V_{max} the maximum velocity, K_M the Michaelis constant, and $[S]$ the substrate concentration.

$$v = \frac{V_{max}[S]}{K_M + [S]} \quad (1)$$

GSTF9 FOX assay with GSH and GSO_3

Ferrous oxidation-xylenol orange (FOX) assay was used to monitor the peroxidase activity of GSTF9.[39] The assay was performed as described by Tossounian et al.[12] Briefly, the reaction mixture included 50 μM $GSTF9_{red}$ or $GSTF9_{ox}$, 1 mM GSH, and 150 μM H_2O_2 in 100 mM potassium phosphate buffer at pH 6.4, which was incubated at room temperature (RT). At three time points (0, 15, and 30 min), 10 μL of the sample was mixed with 490 μL of the FOX assay mixture and incubated in the dark. After 30 min, SpectraMax340PC spectrophotometer (Molecular Devices) was used to measure the absorption at 560 nm. To determine the effect of GSO_3 on the glutathione peroxidase activity of GSTF9, the same procedure was followed with the addition of 0.5 mM GSO_3. As background, the reaction mixture without enzyme was used. A reaction mixture containing 1 mM GSO_3 was also used as a control. Glutathione peroxidase activity of GSTF9 was also tested by replacing H_2O_2 (200 μM) with two hydrophobic peroxides, cumene (200 μM) or tert-butyl hydroperoxide (200 μM). Three independent measurements were performed and the data representing the $\Delta[peroxide]_{ox\text{-}red}$ versus ALogP value of H_2O_2 (−0.18), tert-butyl hydroperoxide (0.79), and CuOOH (2.02) was plotted using GraphPad prism7. The AlogP values were obtained from ChEMBL.

GSTF9-GSO_3 inhibition assays

To determine the GSTF9 inhibition by GSO_3, the SpectraMax340PC spectrophotometer (Molecular Devices) was used, where increasing concentrations of GSO_3 (0, 25, 50, 100, 200, 300, 400, and 500 μM) were added to the reaction mixture containing 0.4 μM reduced GSTF9, 0.5 mM GSH and 3.8 mM CDNB in 250 mM MOPS pH 6.5 and 150 mM NaCl buffer. The reaction started by the addition of CDNB. As background, the reaction mixture without enzyme was used. The inhibition constant for the inactivation of GSTF9 by GSO_3 was determined from the plot of the initial velocities versus the GSO_3 concentration [Eq. (2)]. For all data, two independent measurements were performed and GraphPad prism7 was used to plot the data. In Eq. (2), v_i represents the initial velocity, K_i the inhibition

constant, V the maximum velocity, and [GSO_3] the concentration of inhibitor.

$$v_i = \frac{K_i \times V}{K_i + [GSO_3]} + A \quad (2)$$

GSTF9 thermodynamic parameter determination

GSTF9 thermodynamic parameters were assessed by measuring the initial velocity variation in function of temperature. The reactions were carried out at 17°C, 20°C, 25°C, 30°C, and 37°C in quartz cuvettes using a UV–visible Varian Cary 100 spectrophotometer and were monitored for 180 s with GSTF9 (reduced or oxidized) final concentration 0.2 μM, 0.5 mM GSH, and 3.8 mM CDNB in 250 mM MOPS pH 6.5 and 150 mM NaCl buffer. The values presented correspond to two replicates. Subsequently, the thermodynamic parameters were obtained fitting the data to Arrhenius [Eq. (3)] and Eyring [Eq. (4)] approaches. The Gibbs free energy of activation ($\Delta G^{\#}$) was calculated using Eq. (5). In Eq. (3), E_a represents the reaction activation energy, R, the gas constant (8.314 J mol^{-1} K^{-1}) and A, the product of the collision frequency (Z). For Eq. (4), k_B represents the Boltzmann constant (1.3805×10^{-23} J K^{-1}), h, the Planck's constant (6.6256×10^{-34} J s). For Eq. (5), $\Delta H^{\#}$ and $\Delta S^{\#}$ represent the enthalpy and entropy variation of activation, respectively.

$$\ln k = -\frac{E_a}{R}\frac{1}{T} + \ln A \quad (3)$$

$$\ln\left(\frac{k}{T}\right) = -\frac{\Delta H^{\#}}{R}\frac{1}{T} + \frac{\Delta S^{\#}}{R} + \ln\left(\frac{k_b}{h}\right) \quad (4)$$

$$\Delta G^{\#} = \Delta H^{\#} - T\Delta S^{\#} \quad (5)$$

Mass spectrometric analysis of Met oxidation

For the identification of oxidized Met residues (methionine sulfoxide and methionine sulfone), $GSTF9_{red}$ and $GSTF9_{ox}$ were analyzed by mass spectrometry as described by Tossounian et al.[12]

Acknowledgments

The authors thank the beamline scientist at the Diamond Light Source beamline IO4 for their technical support. Furthermore, they thank Kristof Moonens from VIB-VUB Center for Structural Biology for X-ray data collection on the GSTF9 crystals. They thank Frank Van Breusegem from Ghent University, Belgium for giving us *At-gstF9* plasmid.

Author Contributions

GSTF9 purification was performed by MAT, KW, and IVM. Biochemical, kinetic, and thermodynamic assays were performed by MAT. Crystallization was performed by KW and IVM, and X-ray crystal structures were solved by IVM. Mass spectrometry and data analysis was performed by DV. MAT, IVM, LAR, and JM wrote the manuscript. JM supervised all aspects of the project.

Accession Codes

The structures of $GSTF9_{red}$ (PDB 6EZY), $GSTF9_{H2O2+NaOCl}$ (PDB 6F01), and $GSTF9_{ox}$ (PDB 6F05) have been deposited in the Protein Data Bank.

Conflict of Interest

The authors declare that they have no conflicts of interest with the contents of this article.

References

1. Jacques S, Ghesquiere B, De Bock PJ, Demol H, Wahni K, Willems P, Messens J, Van Breusegem F, Gevaert K (2015) Protein methionine sulfoxide dynamics in *Arabidopsis thaliana* under oxidative stress. Mol Cell Proteom 14:1217–1229.
2. DeRidder BP, Dixon DP, Beussman DJ, Edwards R, Goldsbrough PB (2002) Induction of glutathione S-transferases in *Arabidopsis* by herbicide safeners. Plant Physiol 130:1497–1505.
3. Dixon DP, Hawkins T, Hussey PJ, Edwards R (2009) Enzyme activities and subcellular localization of members of the *Arabidopsis* glutathione transferase superfamily. J Exp Bot 60:1207–1218.
4. Marrs KA, Walbot V (1997) Expression and RNA splicing of the maize glutathione S-transferase Bronze2 gene is regulated by cadmium and other stresses. Plant Physiol 113:93–102.
5. Prade L, Huber R, Bieseler B (1998) Structures of herbicides in complex with their detoxifying enzyme glutathione S-transferase - explanations for the selectivity of the enzyme in plants. Structure 6:1445–1452.
6. Menon D, Board PG (2013) A role for glutathione transferase Omega 1 (GSTO1-1) in the glutathionylation cycle. J Biol Chem 288:25769–25779.
7. Laborde E (2010) Glutathione transferases as mediators of signaling pathways involved in cell proliferation and cell death. Cell Death Differ 17:1373–1380.
8. Sheehan D, Meade G, Foley VM, Dowd CA (2001) Structure, function and evolution of glutathione transferases: implications for classification of non-mammalian members of an ancient enzyme superfamily. Biochem J 360:1–16.
9. Deponte M (2013) Glutathione catalysis and the reaction mechanisms of glutathione-dependent enzymes. Biochim Biophys Acta 1830:3217–3266.
10. Thom R, Dixon DP, Edwards R, Cole DJ, Lapthorn AJ (2001) The structure of a zeta class glutathione S-transferase from *Arabidopsis thaliana*: characterisation of a GST with novel active-site architecture and a putative role in tyrosine catabolism. J Mol Biol 308: 949–962.
11. Thom R, Cummins I, Dixon DP, Edwards R, Cole DJ, Lapthorn AJ (2002) Structure of a tau class glutathione S-transferase from wheat active in herbicide detoxification. Biochemistry 41:7008–7020.
12. Tossounian MA, Van Molle I, Wahni K, Jacques S, Gevaert K, Van Breusegem F, Vertommen D, Young D, Rosado LA, Messens J (2018) Disulfide bond formation

protects *Arabidopsis thaliana* glutathione transferase tau 23 from oxidative damage. Biochim Biophys Acta 1862:775–789.
13. Lee SH, Li CW, Koh KW, Chuang HY, Chen YR, Lin CS, Chan MT (2014) MSRB7 reverses oxidation of GSTF2/3 to confer tolerance of *Arabidopsis thaliana* to oxidative stress. J Exp Bot 65:5049–5062.
14. Wagner U, Edwards R, Dixon DP, Mauch F (2002) Probing the diversity of the *Arabidopsis* glutathione S-transferase gene family. Plant Mol Biol 49:515–532.
15. Horvath E, Bela K, Papdi C, Galle A, Szabados L, Tari I, Csiszar J (2015) The role of *Arabidopsis* glutathione transferase F9 gene under oxidative stress in seedlings. Acta Biol Hung 66:406–418.
16. Mashiyama ST, Malabanan MM, Akiva E, Bhosle R, Branch MC, Hillerich B, Jagessar K, Kim J, Patskovsky Y, Seidel RD, Stead M, Toro R, Vetting MW, Almo SC, Armstrong RN, Babbitt PC (2014) Large-scale determination of sequence, structure, and function relationships in cytosolic glutathione transferases across the biosphere. PLoS Biol 12:e1001843.
17. Wadington MC, Ladner JE, Stourman NV, Harp JM, Armstrong RN (2009) Analysis of the structure and function of YfcG from Escherichia coli reveals an efficient and unique disulfide bond reductase. Biochemistry 48:6559–6561.
18. Stourman NV, Branch MC, Schaab MR, Harp JM, Ladner JE, Armstrong RN (2011) Structure and function of YghU, a nu-class glutathione transferase related to YfcG from Escherichia coli. Biochemistry 50: 1274–1281.
19. Nutricati E, Miceli A, Blando F, De Bellis L (2006) Characterization of two *Arabidopsis thaliana* glutathione S-transferases. Plant Cell Rep 25:997–1005.
20. Eftink MR, Anusiem AC, Biltonen RL (1983) Enthalpy-entropy compensation and heat capacity changes for protein-ligand interactions: general thermodynamic models and data for the binding of nucleotides to ribonuclease A. Biochemistry 22:3884–3896.
21. Moons A (2005) Regulatory and functional interactions of plant growth regulators and plant glutathione S-transferases (GSTs). Vitam Horm 72:155–202.
22. Etienne F, Resnick L, Sagher D, Brot N, Weissbach H (2003) Reduction of Sulindac to its active metabolite, sulindac sulfide: assay and role of the methionine sulfoxide reductase system. Biochem Biophys Res Commun 312:1005–1010.
23. Axarli I, Dhavala P, Papageorgiou AC, Labrou NE (2009) Crystal structure of *Glycine max* glutathione transferase in complex with glutathione: investigation of the mechanism operating by the Tau class glutathione transferases. Biochem J 422:247–256.
24. Axarli I, Georgiadou C, Dhavala P, Papageorgiou AC, Labrou NE (2010) Investigation of the role of conserved residues Ser13, Asn48 and Pro49 in the catalytic mechanism of the tau class glutathione transferase from *Glycine max*. Biochim Biophys Acta 1804:662–667.
25. Labrou NE, Papageorgiou AC, Pavli O, Flemetakis E (2015) Plant GSTome: structure and functional role in xenome network and plant stress response. Curr Opin Biotechnol 32:186–194.
26. Dixon DP, Lapthorn A, Edwards R (2002) Plant glutathione transferases. Genome Biol 3:REVIEWS3004.
27. Huang J, Khan Niazi A, Young D, Rosado LA, Vertommen D, Bodra N, Abdelgawwad MR, Vignols F, Wei B, Wahni K, Bashandy T, Bariat L, Van Breusegem F, Messens J,JPR (2017) Self-protection of cytosolic malate dehydrogenase against oxidative stress in *Arabidopsis*. J Exp Bot https://doi.org/10.1093/jxb/erx396.
28. Gustavsson N, Kokke BP, Anzelius B, Boelens WC, Sundby C (2001) Substitution of conserved methionines by leucines in chloroplast small heat shock protein results in loss of redox-response but retained chaperone-like activity. Protein Sci 10:1785–1793.
29. Balog EM, Lockamy EL, Thomas DD, Ferrington DA (2009) Site-specific methionine oxidation initiates calmodulin degradation by the 20S proteasome. Biochemistry 48:3005–3016.
30. Flury T, Wagner E, Kreuz K (1996) An inducible glutathione S-transferase in soybean hypocotyl is localized in the apoplast. Plant Physiol 112:1185–1190.
31. Gronwald JW, Plaisance KL (1998) Isolation and characterization of glutathione S-transferase isozymes from sorghum. Plant Physiol 117:877–892.
32. Manta B, Hugo M, Ortiz C, Ferrer-Sueta G, Trujillo M, Denicola A (2009) The peroxidase and peroxynitrite reductase activity of human erythrocyte peroxiredoxin 2. Arch Biochem Biophys 484:146–154.
33. Toppo S, Flohe L, Ursini F, Vanin S, Maiorino M (2009) Catalytic mechanisms and specificities of glutathione peroxidases: variations of a basic scheme. Biochim Biophys Acta 1790:1486–1500.
34. Du X, Li Y, Xia YL, Ai SM, Liang J, Sang P, Ji XL, Liu SQ (2016) Insights into protein-ligand Interactions: mechanisms, models, and methods. Int J Mol Sci 17:E144.
35. Loftfield RB, Eigner EA, Pastuszyn A, Lovgren TNE, Jakubowski H (1980) Conformational-changes during enzyme catalysis - Role of water in the transition-state. Proc Natl Acad Sci USA 77:3374–3378.
36. Lonhienne T, Gerday C, Feller G (2000) Psychrophilic enzymes: revisiting the thermodynamic parameters of activation may explain local flexibility. Biochim Biophys Acta 1543:1–10.
37. Habig WH, Pabst MJ, Jakoby WB (1974) Glutathione S-transferases. The first enzymatic step in mercapturic acid formation. J Biol Chem 249:7130–7139.
38. Tossounian MA, Pedre B, Wahni K, Erdogan H, Vertommen D, Van Molle I, Messens J (2015) *Corynebacterium diphtheriae* methionine sulfoxide reductase a exploits a unique mycothiol redox relay mechanism. J Biol Chem 290:11365–11375.
39. Jaeger J, Sorensen K, Wolff SP (1994) Peroxide accumulation in detergents. J Biochem Biophys Methods 29:77–81.